*Magnetohydrodynamics, Vol. 30, No. 4, 1994*

# SOME ASPECTS OF LMMHD TWO-PHASE FLOW: MHD GENERATOR CONFIGURATION

**S. Eckert,[1] G. Gerbeth,[1]**
**J.-P. Thibault,[2] and G. Mihalache[2]**

*The influence of an external magnetic field on LMMHD two-phase flows in vertical rectangular ducts has been examined. The goal of our work is the construction of models that are able to predict the average behavior of the flow as well as models that are relatively easy to survey and to handle. Results regarding the slip ratio obtained from a bubbly flow model are compared with experimental data obtained from measurements at the mercury-air facility. In the case of an applied magnetic field, discrepancies between model and experiment are obtained giving an indication of the imperfection of the present state of the model. The crucial point is the validation of the semi-empirical closure laws involved in the LMMHD two-phase flow models. In the present state of the experiments the influence of the void fraction on the apparent electrical conductivity of the two-phase flow has been investigated. The results obtained from the mercury-air facility of LEGI-IMG are intermediate between the relations given by Maxwell and Petrick and Lee, respectively.*

## Introduction

Profound knowledge on LMMHD two-phase flow plays an important role in a variety of technological applications, in particular, in the design of liquid-metal MHD generators. However, the highly empirical nature of two-phase flow analysis gives little hope for the prediction of MHD two-phase flows without extensive experimental data. Therefore, a common program is developed which includes experimental as well as modeling aspects.

First results have been obtained from measurements at the mercury-air facility of LEGI-IMG. Experimental activities are also planned for the sodium-argon facility of FZR. Experiments on both test loops allow us to observe LMMHD two-phase flow phenomena in very different parameter regions (see Table 1).

The measurements should be accompanied by the development of theoretical models. In fact, a bubbly flow and a two-fluid model have been developed in order to meet the requirements of both facilities. The bubbly flow conditions are fullilled very well on the sodium-argon facility, while the two-fluid model is supposed to be a good approach for the description of two-phase flows with a higher gas content as in the case of the LEGI mercury-air facility (Table 1).

However, it will be very interesting to apply the codes crosswise and to compare the results directly in order to find the limitations of each model. The present work is based mainly on experimental data obtained at the mercury-air facility of LEGI-IMG and the one-dimensional bubbly flow model of FZR.

The closure of any two-phase flow model is necessarily based on semi-empirical closure laws. One of the key questions of LMMHD two-phase flow is the validation of these closure laws. As a matter of fact, they are well established for ordinary two-phase flow, but in the case of LMMHD they still remain uncertain. For instance the modification of interfacial momentum transfer (i.e., interfacial dragging) is important. The additional equations (i.e., Ohm's law) needed for the computation of current density and Lorentz forces are necessarily based on a closure law for the apparent electrical conductivity of the two-phase flow.

[1]Research Center Rossendorf (FZR), Germany.
[2]Laboratoire des Écoulements Géophysiques et Industriels, Institut de Mécanique de Grenoble (LEGI-IMG), France.

Published in Magnitaya Gidrodinamika, No. 4, pp. 664-677, October-December, 1994. Original article submitted January 13, 1995.

0024-998X/94/3004-0559$12.50  

TABLE 1. Physical Properties and Dimensionless Parameters for Both Facilities

| | Mercury-air facility of IMG | Sodium-argon facility of FZR |
|---|---|---|
| Temperature [°C] | 17 | 200 |
| $\rho_l$ [kg/m$^3$] | 1.36 $10^4$ | 9.03 $10^2$ |
| $\mu_l$ [N/sm$^2$] | 1.50 $10^{-3}$ | 4.57 $10^{-4}$ |
| $\sigma_l$ [1/Ωm] | 1.00 $10^6$ | 7.46 $10^6$ |
| p (at channel inlet) [Pa] | 5.40 $10^5$ | 2.20 $10^5$ |
| $\rho_g$ [kg/m$^3$] | 6.24 | 2.42 |
| $\beta = Q_g/Q_l$ | 0.24 | 0.015 |
| $d_H$ [m] | 0.0175 | 0.0474 |
| Re | 240000 | 100000 |
| $Re_b$ | 65000 | 4700 |
| Ha | 350 ($B_0$=0.77T) | 2700 ($B_0$=0.45T) |
| $Ha_b$ | 120 | 350 |
| N | 0.5 | 80 |
| $N_b$ | 0.22 | 25 |

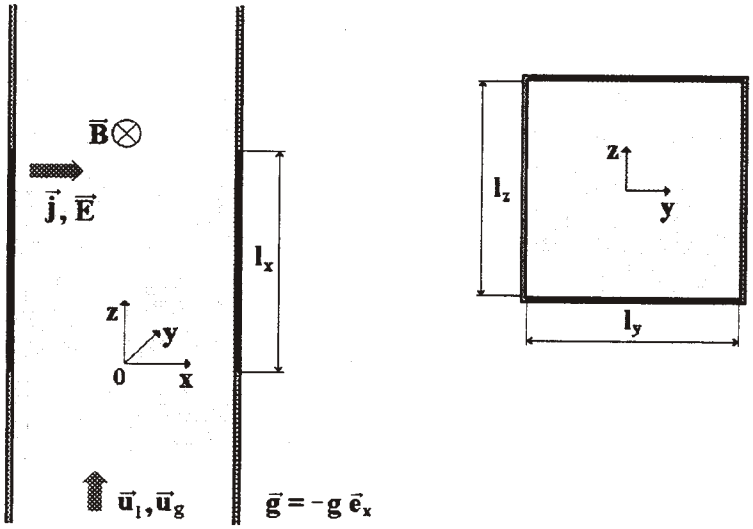


Fig. 1. MHD channel configuration of the considered model.

Presently, the numerical modeling effort is aimed to predict the effects of various initial values on the parameters of a bubbly flow. The analysis is focused on the influence of a magnetic field on the slip ratio because of the decisive role of the mean slip on the overall generator efficiency. Since the pressure drop in a LMMHD generator is two or three orders of magnitude higher than in ordinary two-phase flows, the loss of energy that results from slip becomes very important.

**Description of the Bubbly Flow Model**

Our model is one-dimensional and restricted to the bubbly flow regime. In order to describe the motion of a multitude of bubbles in a liquid metal we partly follow and extend the papers of Kamiyama [1] and Mond and Sukoriansky [2] which are founded on the well-known van Wijngarden model of bubbly flow.

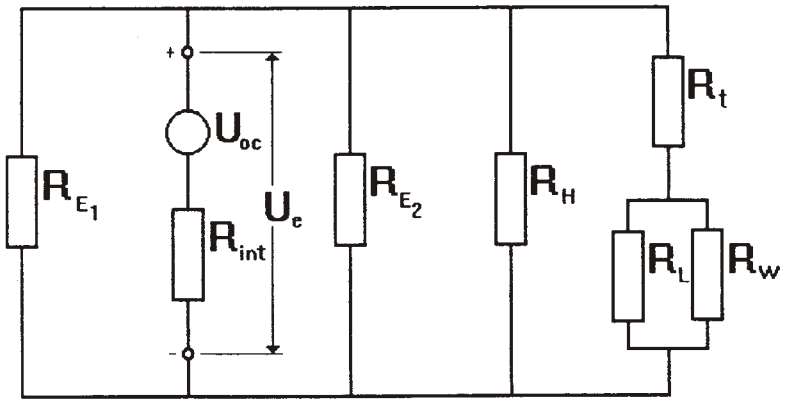


Fig. 2. Equivalent electrical circuit.

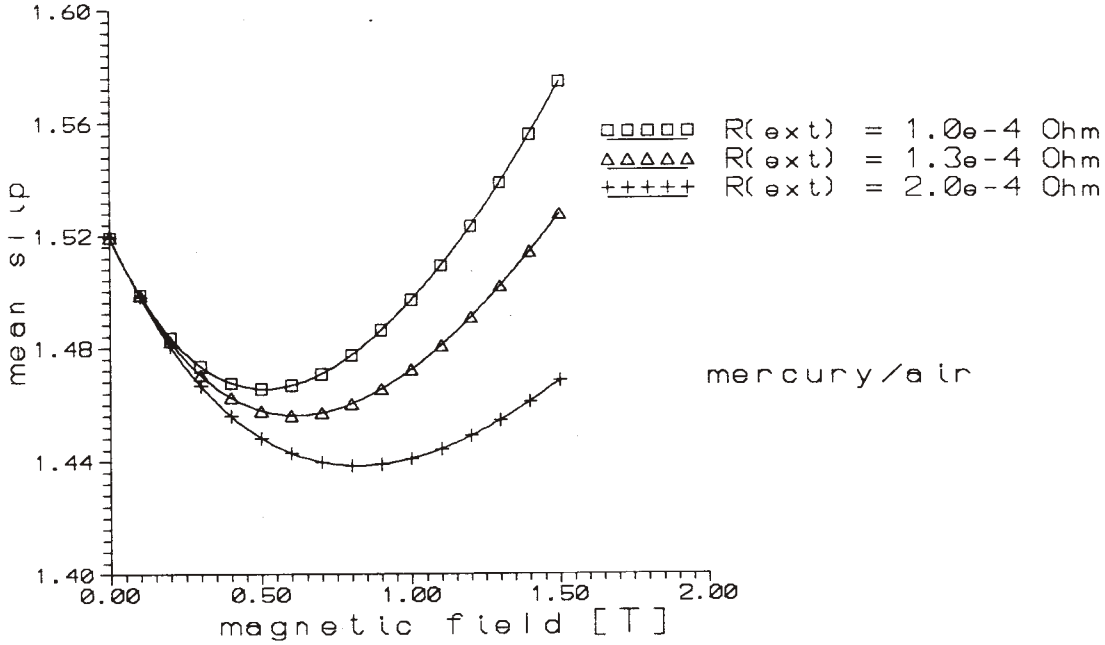


Fig. 3. Mean slip as a function of the transverse magnetic field with the external resistance as parameter.

We consider a vertical upwards flow of a liquid metal in a rectangular duct exposed to an external magnetic field. The channel cross section is assumed to be constant. The geometry of the problem is shown in Fig. 1 for the case of a transverse field.

The fluid and gas flow is assumed to be in the x-direction only. All variables are functions of x only and involved in the code as cross-section averaged values. A proper consideration of the cross-sectional averaging process is possible by introduction of the so-called correlation coefficients (see Yakhot and Branover [3]; Saito et al. [4]). However, this step is not included in the first calculations, but it will be done as soon as the required experimental data are available.

In the case of a transverse applied field the induced magnetic field is assumed to be negligible, with the result that $\mathbf{B}$ has only a y-component, $\mathbf{B} = (0, B_0, 0)$. The B-field strength is constant in the domain between the electrodes and decreases exponentially outside this region. The electrodes on both sides are perfect conductors. Therefore, the current density $\mathbf{j}$ as well as the induced electrical field $\mathbf{E}$ (where $\vec{j} = \sigma_t(\vec{E} + \vec{u} \times \vec{B})$) have only one component in the z-direction. From $\nabla \mathbf{E} = 0$ and $\nabla \times \mathbf{E} = 0$ the electrical field $\mathbf{E}$ is constant in space.

Further assumptions are the following:

- The flow is isothermal due to the large heat capacity of the liquid metal.
- The flow is steady.
- The pressure difference between gas and the surrounding fluid is neglected.
- The gas phase is treated as ideal gas.

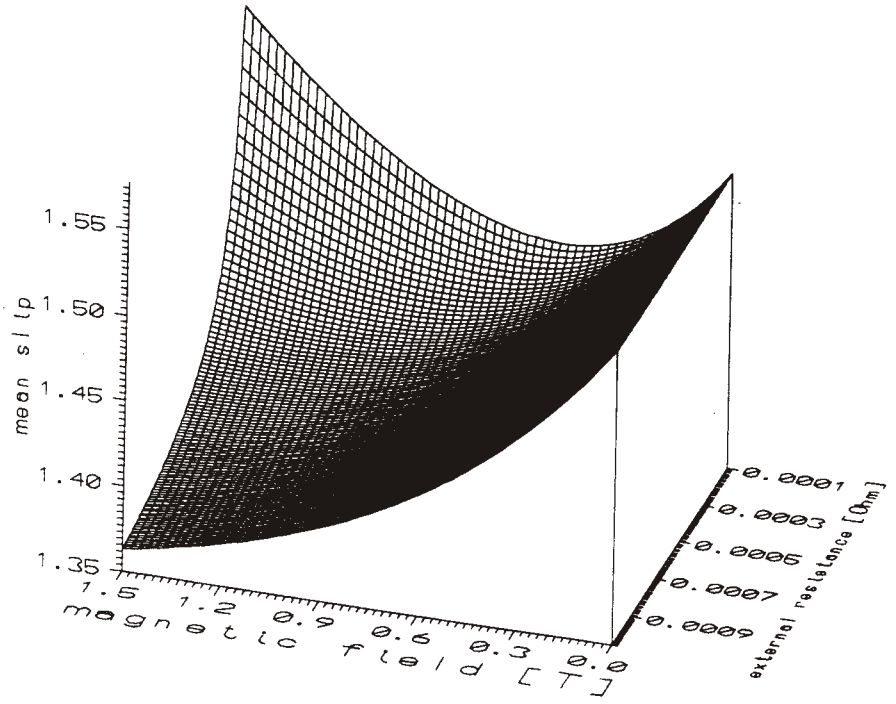


Fig. 4. Mean slip as a function of the transverse magnetic field and the external resistance.

- The gas phase consists of spherical bubbles of mean radius r(x).
- There is no mass transfer between the phases (i.e., no evaporation or condensation).
- The effects of aggregation or breakup of bubbles are neglected.

From the above assumptions the final system of equations is given by:

*continuity*:

$$\frac{d[(1-\alpha)u_l]}{dx}=0 \quad , \quad \frac{d(\alpha\rho_g u_g)}{dx}=0 \tag{1}$$

*combined momentum equation*:

$$\alpha\rho_g u_g\left(\frac{du_g}{dx}\right)+(1-\alpha)\rho_l u_l\left(\frac{du_l}{dx}\right)=-\frac{dp}{dx}-\left[\alpha\rho_g+(1-\alpha)\rho_l\right]g-f_R+(\vec{j}\times\vec{B})_x \tag{2}$$

*equation of motion of a single bubble:*

$$\frac{d(\rho_g V_b u_g)}{dt}=-V_b\left(\frac{dp}{dx}\right)-\rho_g V_b g-F_D-F_{VM} \tag{3}$$

where $F_D=0.5\rho_l\pi r^2 C_D(u_g-u_l)\left|u_g-u_l\right|$ is the drag force

$F_{VM}=0.5\rho_l u_g\dfrac{d\left[V_b(u_g-u_l)\right]}{dx}$ is the virtual mass force

*bubble's mass conservation and equation of state*:

$$\rho_g r^3=const., \qquad \frac{p}{\rho_g}=const. \tag{4}$$

This system of equations is complete if the corresponding closure laws for the frictional force density $f_R$, the apparent electrical conductivity of the two-phase flow $\sigma_t$, the load factor K(x), and the drag coefficient of the bubble $C_D$ are specified.

In the numerical code this is realized by:

- A Lockhart–Martinelli modeling [5] is used to specify the value of $f_R$.

• The local two-phase electrical conductivity is assumed to be a function of the void fraction only and can be expressed by

a) the Maxwell relation

$$\sigma_t = \sigma_l \frac{2(1-\alpha)}{2+\alpha} \tag{5a}$$

b) the Petrick and Lee relation

$$\sigma_t = \sigma_l \exp(-3.8\alpha) \tag{5b}$$

• The load factor is needed to formulate the Lorentz term in the momentum equation.

The current density is given by Ohm's law

$$j_z = \sigma_t (E_z + u_l B_0) \tag{6}$$

($E_z < 0$ in the generator case, $E_z > 0$ in the pump case).

Equation (6) can be rewritten as

$$j_z = \sigma_t u_l B_0 [1 - K(x)] \tag{7}$$

where the definition of the load factor is given by $K(x) = -(E_z/u_l B_0)$.

The voltage between the electrodes is obtained from

$$U_e = -\int_{-\frac{l_z}{2}}^{\frac{l_z}{2}} E_z dz = -E_z l_z \ . \tag{8}$$

Calculating the total current via

$$I_t = \int_0^{l_x} \int_{-\frac{l_y}{2}}^{\frac{l_y}{2}} j_z(x)\, dx dy \tag{9}$$

the load voltage can also be written as $U_e = I_t R_{ext}$ where $R_{ext}$ represents the total electric load of the MHD channel. If a constant load factor is defined in the following manner

$$K_0 = K(x) \frac{u_l}{u_{l(x=0)}} = \frac{U_e}{u_{l(x=0)} B_0 l_z} = \frac{I_t R_{ext}}{u_{l(x=0)} B_0 l_z} \tag{10}$$

the Lorentz term can ultimately be written as

$$\left(\vec{j} \times \vec{B}\right)_x = -\sigma_t B_0^2 (u_l - K_0 u_{l(x=0)}) \ . \tag{11}$$

• A semi-empirical closure law [2] is used for relating the drag coefficient $C_D$ to that of a single bubble $C_{Ds}$

$$C_D = C_{Ds} (1-\alpha)^4 \tag{12}$$

The single bubble drag is given by [6]

$$C_{Ds} = C\ (1 + \sqrt{N_b}) \tag{13a}$$

in the case of a transverse field $\mathbf{B} = B_0 \mathbf{e}_y$, and

$$C_{Ds} = 0.33 \sqrt{N_b} \tag{13b}$$

in the case of a longitudinal field $\mathbf{B} = B_0 \mathbf{e}_x$. Here C is the single bubble drag without magnetic field taken from the standard drag curve for the corresponding value of the local bubble Reynolds number $Re_b$.

Figure 2 shows the equivalent circuit of an MHD generator as an electrical device. The MHD duct acts as a simple d.c. source with the internal resistance $R_{int}$ which is connected with an exterior resistance $R_{ext}$. In the first calculations $R_{ext}$

is assumed to be equal to $R_L$ (load resistance + connections). Moreover, closing of the electrical circuit is also possible via $R_H$, the resistance of the Hartmann layers, and $R_W$, the resistance of the channel wall, if the finite electrical conductivity of the electrodes is taken into account. $R_t$ denotes the contact resistance between the liquid metal and the channel wall.

End effects are taken into account in the following way: The conducting fluid in the regions upstream and downstream of the magnetic field acts as an electrical shunt $R_E$ in parallel with the fluid that is inside the magnetic field region. The method of end resistance modeling is derived from a paper of Sutton et al. [7]. Accordingly, $R_E$ is given by

$$R_E = \frac{\pi}{\sigma_l l_y (\ln 2 - \zeta)} \tag{14}$$

with

$$\zeta = \gamma^{-1}\left[1 - \pi^{-\frac{1}{2}}\Gamma(0.5\gamma + 0.5)/\Gamma(0.5\gamma + 1)\right]$$
$$\gamma = l_y/\pi x_e$$

if the B-field outside the electrodes can be written as $B = B_0\exp\{-[|x| - x_0]\}/x_e\}$. $R_E$ consists of two parts at the inlet and at the outlet, respectively (Fig. 2). $R_{ext}$ can consequently be calculated as follows:

$$\frac{1}{R_{ext}} = \frac{1}{R_E} + \frac{1}{R_H} + \frac{1}{R_t + \dfrac{R_L R_W}{R_L + R_W}} \tag{15}$$

**Results from the Calculations**

The system of equations is numerically solved by using a Runge–Kutta algorithm. Our interest is focused on the mean slip ratio defined by

$$\bar{S} = \frac{1}{l_x}\int_0^{l_x} \frac{u_g(x)}{u_l(x)}dx \tag{16}$$

Moreover, the results of the slip at a specified x-position (probe position in the experiment) and the pressure drop have been evaluated.

For each run the values of the liquid and the gaseous flow rate, the pressure, the bubble radius, and the liquid velocity are specified at the channel inlet (x = 0).

The void fraction and gas velocity at x = 0 are calculated from the following relations:

$$\alpha_{(x=0)} = 1 - \frac{Q_l}{u_{l(x=0)}A} \quad ; \quad u_{g(x=0)} = \frac{Q_{g(x=0)}}{\alpha_{(x=0)}A} \tag{17}$$

In the case where the external resistance $R_{ext}$ is given, $K_0$ has to be determined by the requirement that the total current $I_t$ obtained from Eq. (10) and the value of $I_t$ derived by integration of Eq. (9) must yield the same value. A shooting method is used for the solution of this problem in the code.

The influence of an external transverse magnetic field on the mean slip is determined by two opposite effects:

1) The magnetic field has a braking effect on the liquid metal.

2) The magnetic field enhances the drag coefficient of a single bubble [see Eq. (13a)].

Both effects are reflected in the shape of the curves shown in Fig. 3. They are typical for the results obtained from the calculations for the case of a transverse magnetic field. This figure shows the dependence of the mean slip on the field strength with the external resistance as parameter. The first part of the curves is determined by the second effect, while in the second part the braking effect becomes dominant. The external resistance is an important parameter. With increasing external resistance the Lorentz term decreases, and for relatively large resistances the braking effect disappears (see Fig. 4).

A very interesting situation appears for the LMMHD two-phase flow in a longitudinal magnetic field. In this case $\vec{u}_l \times \vec{B}$ becomes zero and, in principle, we have no braking effect on the liquid metal. Thus, results obtained from our model

TABLE 2. Comparison between Results Obtained from Measurements on the Mercury/Air Facility and Numerical Calculations, Respectively

| Value at probe position | B = 0 T | | B = 0.77 T | |
|---|---|---|---|---|
| | exper. | calc. | exper. | calc. |
| Slip ratio S | 1.56 | 1.53 | 1.83 | 1.51 |
| Liquid velocity $u_l$ [m/s] | 1.34 | 1.35 | 1.11 | 1.17 |
| Void fraction $\alpha$ | 0.15 | 0.16 | 0.16 | 0.19 |

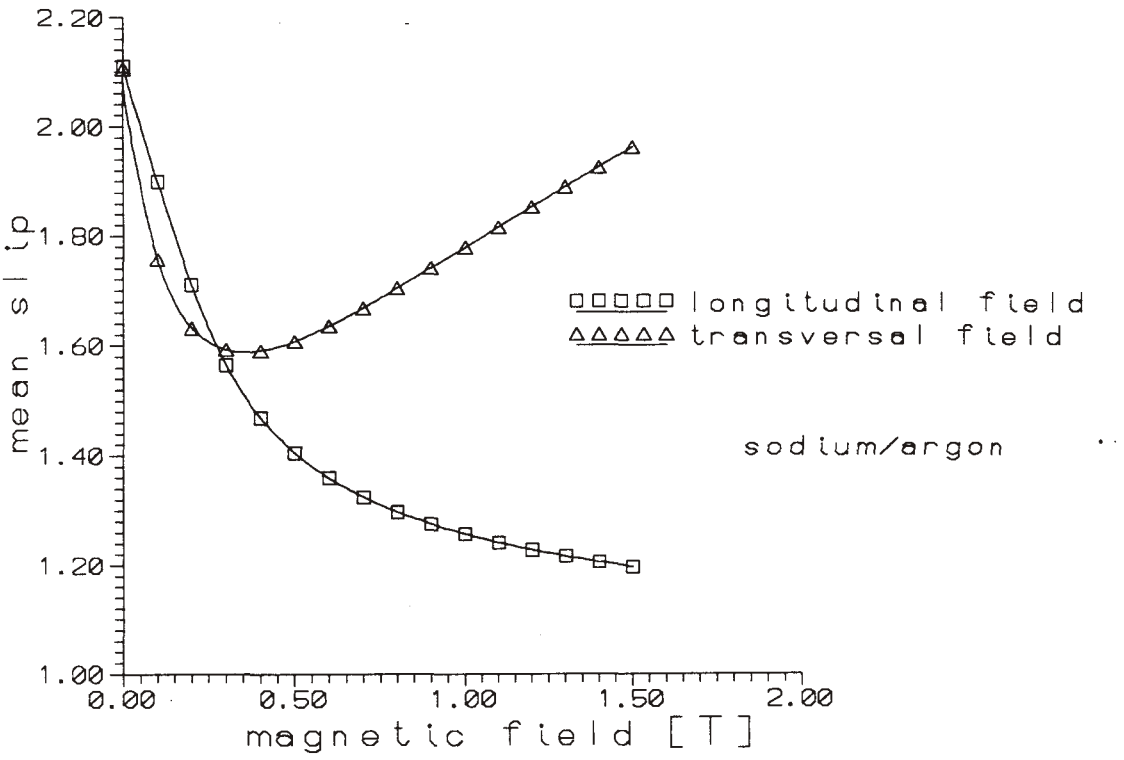


Fig. 5. Mean slip as a function of the transverse and the longitudinal magnetic fields, respectively.

show a monotonous decrease of the mean slip with increasing magnetic field for the case of a sodium-argon flow (see Fig. 5). It would be very interesting to check this result in an experiment.

**Comparison Model – Experiment**

Table 2 shows some results obtained from experimental runs without magnetic field and with a magnetic field of 0.77 T, respectively [8], compared to the corresponding results from the bubbly flow model.

In the case without magnetic field we note a good agreement, while in the other case an important discrepancy between the results is visible. We detect that the model and the experiment do not agree. There are no bubbly flow conditions in this experiment. According to a flow map given by Hewitt and Roberts [9] a plug flow regime has to be expected. Moreover, the absence of electrodes is also in contradiction to the assumptions of the model.

We have tried to specify in more detail the influence of uncertainties of the closure laws on the numerical results. To our opinion, consideration of a bubbly flow instead of the more realistic plug flow leads to an overestimation of the drag coefficient, because of the greater gas volume of a plug compared to a corresponding bubble with nearly the same interface to the liquid metal in the flow direction. Moreover, relating the drag coefficient of the two-phase flow to that of a single bubble causes an additional error. In this connection a confinement effect due to the channel walls was not considered. For these reasons an estimation of the uncertainty of the drag modeling up to 50% seems to be realistic. These inaccuracies would cause a spread of the slip results in the range from 1.5-1.9 approximately.

A modification of other closure laws (for example, to model the apparent electrical conductivity we used the Maxwell relation as well as the relation given by Petrick and Lee) did not lead to such significant changes in the slip results. Therefore, the modeling of the interfacial drag can be identified as the crucial point. The measurements at the sodium-argon facility of FZR will be important, because under these loop conditions a pure bubbly flow can be expected. Thus, a better comparison between the bubbly flow model and the experiment will be possible. For a description of LMMHD two-phase flows with higher gas contents as in the case of the LEGI mercury-air loop, the following ways could be successful:

- application of the two-fluid model
- replacing the closure law of the interfacial drag in the present bubbly flow model by a corresponding relation valid for a plug flow.

Moreover, another aspect could be the limitation of a one-dimensional model. In the one-dimensional model naturally an equal distribution over the cross section of the void fraction is assumed, or in other words the distribution parameter introduced by Zuber and Findley [10] (drift flux model) is unity. Generally, this condition is not fulfilled in the experiment. However, before we can discuss the influence of the void fraction distribution on the mean slip ratio in detail, it will be necessary to collect more experimental data regarding the profiles of the void fraction and the liquid velocity.

## Experimental Measurements

As already mentioned, the closure of any two-phase flow model is necessarily based on semi-empirical closure laws. Thus, in the frame of our collaboration, we decided to combine our experimental equipment to improve the level of knowledge in the field of MHD two-phase flow.

The facility of LEGI-IMG uses a mercury-air two-phase flow passing through a 0.9 m transversal electromagnet ($B_{max}$ = 1.1 T) in a rectangular vertical test section (7 × 1 $cm^2$). The facility of FZR uses a sodium-argon two-phase flow passing through a 0.32 m transverse electromagnet ($B_{max}$ = 0.45 T) in a rectangular test section (5 × 4.5 $cm^2$). The comparison of these two experiments is displayed in Table 1. It is based on a selection of dimensionless parameters which refer either to the entire flow, with the hydraulic diameter of the test section as length scale, or to the local two-phase flow behavior with a typical bubble radius as length scale. Table 1 shows that the two pairs considered are really complementary because they have a high density and a moderate conductivity (mercury-air) and, respectively, a low density and a high conductivity (sodium-argon). Consequently the mercury-air tends to behave as an ordinary two-phase flow regarding the velocity profile (moderate interaction parameter); on the contrary, the sodium-argon tends to be strongly controlled by the electromagnetic forces (high interaction parameter).

Regarding two-phase flow aspects, the void fraction in the mercury-air facility can be higher than 30%; on the other hand it is presently limited to few % on the sodium-argon. Finally the electrical behavior is as follows: the mercury-air facility includes a Faraday generator, the electrode length is 0.9 m as well as the electromagnet length, the electrode gap is 7 cm (constant), and the magnetic gap of the flow is 1 cm (constant). The sodium-argon comprises presently an ordinary (no electrode) rectangular test section with almost insulating walls.

The present status of possible measurements of the sodium-argon facility is limited; thus, we will discuss here only the mercury-air measurement techniques. Our experimental objective is to measure simultaneously electrical and thermohydraulic quantities of a two-phase flow submitted or not submitted to a transverse magnetic field. In this phase of the experimental program our aim is to measure the electrical conductivity of the two-phase mixture.

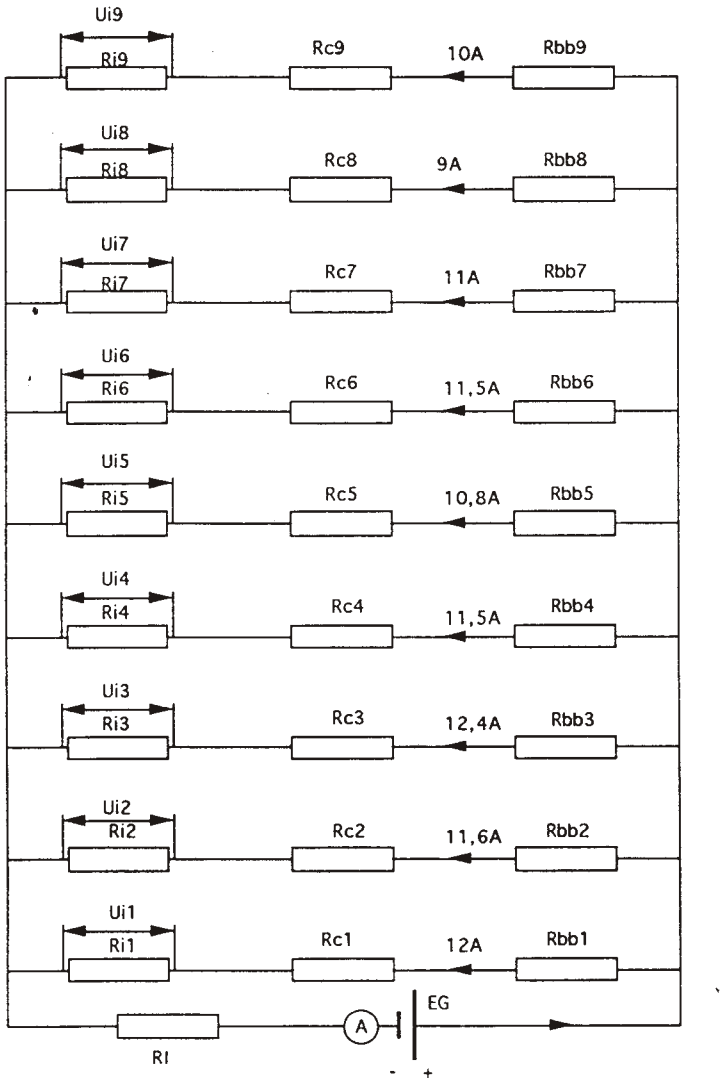


Fig. 6. Electrical scheme of the experimental facility.

The present LEGI-IMG facility consists of a loop using mercury and air as working fluids. The test section includes nine 0.1 m length pairs of electrodes connected to an electric load.

Due to gas injection the apparent density decreases in the upcomer (including the test section); in the downcomer (after separation) the flow is only liquid. Thus the flow in the loop is maintained by natural circulation.

This flow mechanism provides a liquid flow rate of about 8-10 kg/sec. The volumetric quality $\beta$ is between 0.2-0.45. The mercury-air mixture temperature is 12-14°C (285-287 K) and the absolute pressure inside the generator is 166-511 kPa. The pressure drop along the generator varied between 100 and 120 kPa. The thermohydraulic measurements consist of temperature, pressure, and fluid flow rate. The mercury flow rate was measured with a classical electromagnetic flow meter, and the air flow rate, with a rotameter.

The electrical scheme is shown in Fig. 6. The electrical measurements consist of total current (using a calibrated shunt resistance of 1 m$\Omega$), voltage drop on each bus bar (connection between electrodes and load resistance), and voltage drop on internal flow ($U_i$). For $U_i$ we use measuring electrodes which are in direct contact with the two-phase flow. The values

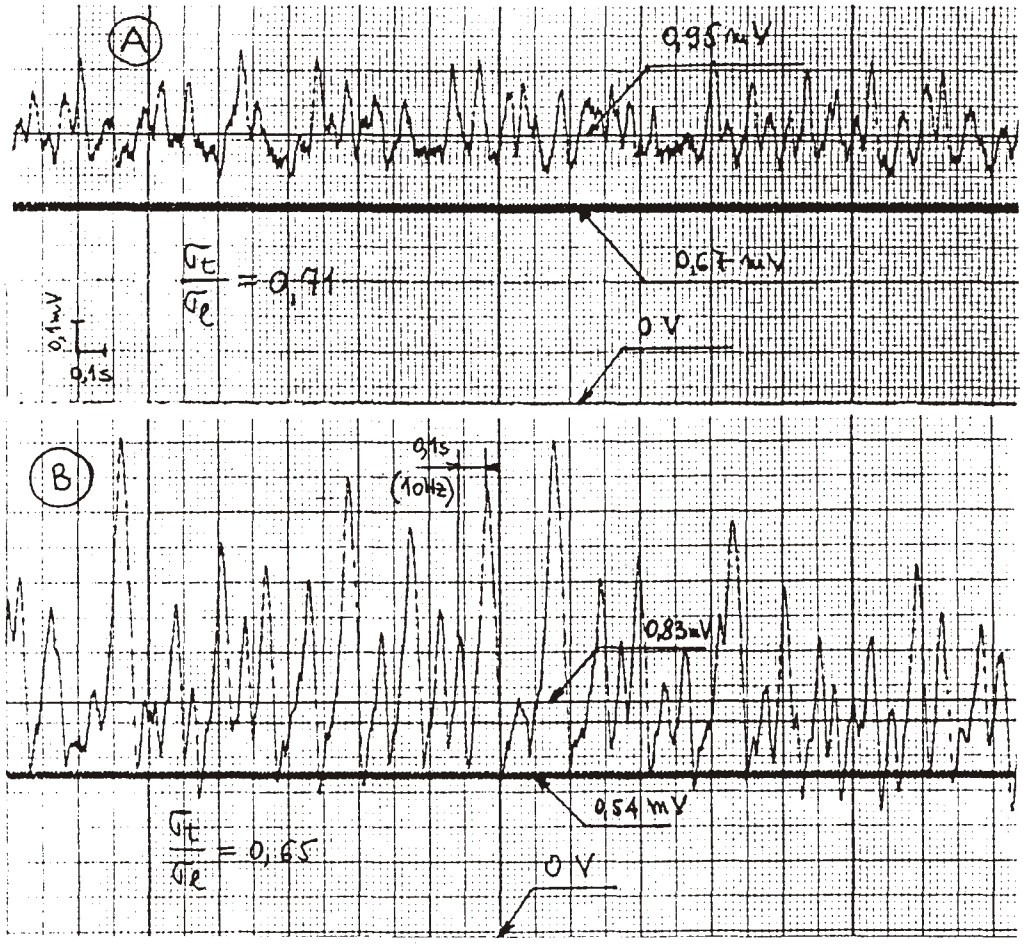


Fig. 7. Recorded voltage drop without gas (low level) and with gas (high level) at two positions of the test section, respectively. A) 0.15 m from inlet, average pressure 500 kPa, average volumetric quality 0.26; B) 0.85 m from inlet, average pressure 385 kPa, average volumetric quality 0.32.

for the resistance are: for the bus bars about $R_{bb} = 175\ \mu\Omega$, for the load resistance $R_l = 500\ \mu\Omega$, for the internal resistance of the pure liquid flow about 70 $\mu\Omega$. Using an external electric source of direct current (DC) we provided for the whole generator a total current of 100 A distributed between electrodes as shown in Fig. 6. The agreement between calculated bus bar currents and the total current (measured) is better than 1%. In our electrical conditions the distribution of bus bar currents is not modified by the two-phase flow because the added internal resistance (due to the gas) is small compared to the external resistance. This aspect was experimentally verified by measuring the voltage drop on each bus bar. That is why the measurements of the two-phase flow conductivity and pure liquid conductivity were made as follows:

$$\begin{aligned} &U_i(l)=R_i(l)I=L/(\sigma(l)S)I \\ &U_i(t)=R_i(t)I=L/(\sigma(t)S)I \quad \text{and} \\ &\sigma(t)/\sigma(l)=U_i(l)/U_i(t) \end{aligned} \tag{18}$$

where $R_i(l, t)$ is the internal resistance of pure liquid and two-phase flow, and L, S are the length and area corresponding to the respective flow section (1-9).

The volumetric quality is obtained from liquid and gas flow rate, pressure and temperature measurements combined with an ideal gas state law. Liquid and gas do not have the same velocities, thus the void fraction does not equal the volumetric quality. As direct measurements of these velocities are not available, the only experimental solution is to measure directly the void fraction. Unfortunately the optical probe that we usually use for this purpose is presently not available for technical reasons [8]. Consequently at the moment, the void fraction is estimated from the volumetric quality combined with the velocity slip ratio based on previous measurements and the present computation. There is a very small difference (2%) between

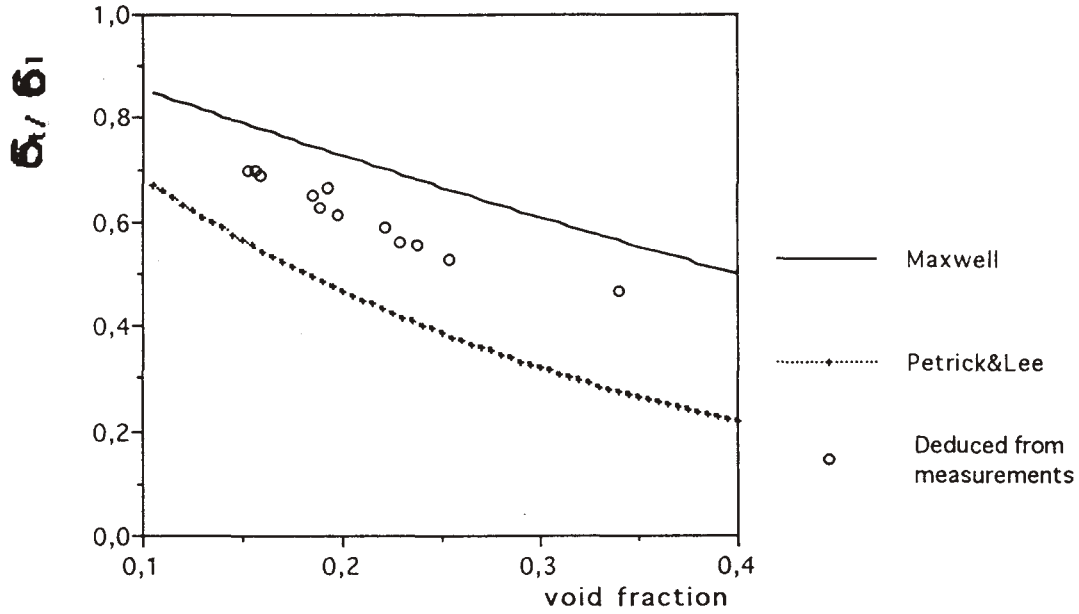


Fig. 8. Comparison of known correlations $\sigma_t(\alpha)$ with values of $\sigma_t(\alpha)$ deduced from measurements, as described.

the slip ratio measured in previous experimental session at LEGI-IMG facility and the FZR numerical model in the case of nonmagnetic field; thus, the area void fraction is practically the same with both results.

Figure 7 is obtained when the flow is supplied by an external DC generator and the magnetic field is off (see Fig. 6). It shows measured electrode signals for various conditions respectively: pure liquid ($U_i(l)$) and two-phase flow ($U_i(t)$) for two different positions in the test section, which means two different volumetric qualities. It clearly demonstrates some fluctuations (3.6 to 13 Hz, with a dominant fluctuation around 10 Hz) due to the local unsteadiness of the two-phase flow. In the next step of measurements a signal analysis will be developed in order to correlate the lower frequencies with the bubble sequence and to correlate higher frequencies with the bubble oscillation.

The average flow voltage drop increases with gas fraction due to decrease in the apparent electrical conductivity of the flow. As a consequence, the two-phase and liquid only conductivity ratio is plotted in Fig. 8. As shown, the measured points are between Maxwell and Petrick and Lee relations. This preliminary analysis needs to be extended, including, first, direct void fraction measurements and, second, an analysis of the magnetic field effect.

## Concluding Remarks

As a preliminary conclusion, we can mention that one-dimensional models are able to predict the average behavior of LMMHD two-phase flows. However, their range of validity is strongly limited by the closure laws involved in the model. The essential problem is the validation and the improvement of the closure laws by means of establishing extensive experimental data bases. This should preferably be achieved by using in the experiments a variety of liquid metals which differ considerably in their properties.

In particular, the determination of the interfacial drag plays the key role for the modeling of the interfacial momentum transfer. The interchange of experiences and ideas regarding the void fraction measurements by means of optical as well as resistivity probes will be a crucial point of future activities.

## Nomenclature

A: cross-sectional area;
B: magnetic field;
$C_D$: drag coefficient;

**Nomenclature (continued)**

| | |
|---|---|
| $d_H$ : | hydraulic diameter; |
| E: | external electric field; |
| $F_D$: | drag force; |
| $F_{VM}$: | virtual mass force; |
| $f_R$: | frictional force density; |
| g: | gravitational acceleration; |
| Ha: | Hartmann number, $B_0 d_H \sqrt{\sigma_l/\mu_l}$ ; |
| $Ha_b$: | bubble Hartmann number, $B_0 2r \sqrt{\sigma_l/\mu_l}$ ; |
| $I_t$: | total current; |
| j: | current density; |
| K: | load factor; |
| $l_x$, $l_y$, $l_z$: | channel extensions; |
| $M_g$, $M_l$: | mass flow rates; |
| $N_b$: | bubble interaction parameter, $Ha_b^2/Re_b$; |
| p: | pressure; |
| $Q_g$, $Q_l$: | volumetric flow rates; |
| Re: | Reynolds number, $\rho_l u_l d_H/\mu_l$; |
| $Re_b$: | bubble Reynolds number, $\rho_l u_l 2r/\mu_l$; |
| R: | electrical resistance; |
| r: | bubble radius; |
| S: | slip ratio; |
| $u_g$, $u_l$: | velocities; |
| $U_e$: | voltage between the electrodes; |
| $V_b$: | bubble volume, $4/3\pi r^3$. |

**Greek characters**

| | |
|---|---|
| $\alpha$: | void fraction; |
| $\beta$: | volumetric quality, $Q_g / (Q_g+Q_l)$; |
| $\rho_g$ ,$\rho_l$: | densities; |
| $\sigma_l$, $\sigma_t$: | electrical conductivities. |

**Subscripts**

| | |
|---|---|
| x, y, z: | quantities for x-, y-, and z-direction, respectively; |
| g: | gaseous phase; |
| l: | liquid phase; |
| t: | Two-phase. |

## REFERENCES


1. Kamiyama, S., "Analysis of two-phase MHD flow in converging-diverging ducts," *Proceedings of the 4th Beer-Sheva Seminar, Jerusalem, Israel 1984,* AIAA, Vol. 100, 1985, pp. 304-316.
2. Mond, M., and Sukoriansky, S., "An analytical model for bubbly flow," *Proceedings of the 4th Beer-Sheva Seminar, Jerusalem, Israel 1984,* AIAA, Vol. 100, 1985, pp. 329-339.
3. Yakhot, A., and Branover, H., "An analytical model of a two-phase liquid metal magnetohydrodynamic generator," *Phys. Fluids*, Vol. 25, No. 3, 1982, pp. 446-451.
4. Saito, M., Inoue, S., and Fujii-e, Y., "Gas-liquid slip ratio and MHD pressure drop in two-phase liquid metal flow in strong magnetic field," *Journal of Nuclear Science and Technology*, Vol. 15, No. 7, 1978, pp. 476-489.

5. Storek, H., and Brauer, H., "Reibungsdruckverlust der adiabaten Gas/Flüssigkeits Strömung in horizontalen und vertikalen Rohren," *VDI Forschungsheft*, No. 599, 1980.
6. Gelfgat, Y. M., Lielausis, O. A., and Szerbinin, E. W., "Liquid metals under the action of electromagnetic fields," Zinatne, Riga, 1976 [in Russian].
7. Sutton, G. W., Hurwitz, H., and Poritsky, H., "Electrical and pressure losses in a magnetohydrodynamic channel due to end current loops," *Trans. AIEE, Part I*, Vol. 80, No. 1, 1962, pp. 687-695.
8. Thibault, J.-P., Seck, B., Cartellier, A., "Liquid-metal magnetohydrodynamic two-phase flow experiment," *Proceedings of the 6th Beer-Sheva Seminar, Jerusalem, Israel 1990,* AIAA, Vol. 148, 1993, pp. 667-677.
9. Hewitt, G. F., and Roberts, D. N., "Studies of two-phase flow patterns by simultaneous X-ray and flash photography," *AERE-M2159*, 1969.
10. Zuber, N., and Findley, J. A., "Average volumetric concentration in two-phase flow systems," *Journal of Heat Transfer*, Vol. 87, 1965, pp. 453ff.